Acta Pharmacologica Sinica (2014) 35: 292–300
 1671-4083/14 $32.00
www.nature.com/aps

Original Article

Hepatic cytochrome P450s play a major role in monocrotaline-induced renal toxicity in mice

Jun YAO, Cheng-gang LI, Li-kun GONG, Chen-chen FENG, Chun-zhu LI, Man GAO, Yang LUAN, Xin-ming QI*, Jin REN*

Center for Drug Safety Evaluation and Research, State Key Laboratory of New Drug Research, Shanghai Institute of Materia Medica, Chinese Academy of Sciences, Shanghai 201203, China

Aim: Monocrotaline (MCT) in plants of the genus *Crotalaria* induces significant toxicity in multiple organs including the liver, lung and kidney. Metabolic activation of MCT is required for MCT-induced toxicity. In this study, we attempted to determine whether the toxicity of MCT in kidney was a consequence of the metabolic activation of MCT in the liver.

Methods: Liver-specific cytochrome P450 reductase-null (Null) mice, wild-type (WT) mice and CYP3A inhibitor ketoconazole-pretreated WT (KET-WT) mice were examined. The mice were injected with MCT (300, 400, or 500 mg/kg, ip), and hepatotoxicity and nephrotoxicity were examined 24 h after MCT treatment. The levels of MCT and its metabolites in the blood, liver, lung, kidney and bile were determined using LC-MS analysis.

Results: Treatment of WT mice with MCT increased the serum levels of alanine aminotransferase, hyaluronic acid, urea nitrogen and creatinine in a dose-dependent manner. Histological examination revealed that MCT (500 mg/kg) caused severe liver injury and moderate kidney injury. In contrast, these pathological abnormalities were absent in Null and KET-WT mice. After injection of MCT (400 and 500 mg/kg), the plasma, liver, kidney and lung of WT mice had significantly lower MCT levels and much higher N-oxide metabolites contents in compared with those of Null and KET-WT mice. Furthermore, WT mice had considerably higher levels of tissue-bound pyrroles and bile GSH-conjugated MCT metabolites compared with Null and KET-WT mice.

Conclusion: Cytochrome P450s in mouse liver play a major role in the metabolic activation of MCT and thus contribute to MCT-induced renal toxicity.

Keywords: monocrotaline; pyrrolizidine alkaloid; hepatic cytochrome P450s; ketoconazole; metabolic activation; hepatic toxicity; renal toxicity

Acta Pharmacologica Sinica (2014) 35: 292–300; doi: 10.1038/aps.2013.145; published online 23 Dec 2013

Introduction

Pyrrolizidine alkaloids (PAs) are naturally occurring phytochemicals that are common constituents of hundreds of plant species around the world. PA-containing plants are likely the most common poisonous plants affecting livestock, wildlife, and humans[1]. Human exposure occurs through the consumption of PA-contaminated food or herbal medicines[2]. As recently as 1995, approximately 6000 people worldwide became victims of PA-induced toxicity[3]. A representative PAs toxin, monocrotaline (MCT), exists in plants of the genus *Crotalaria* and can cause injuries to hepatocytes, liver sinusoidal endothelial cells (LSECs), kidneys, and lungs[4–7].

Metabolic activation is required for MCT-induced toxicity[8]. In general, there are three major metabolic pathways of MCT, N-oxidation, hydrolysis, and dehydrogenation (Figure 1)[1]. The metabolite produced in the final step, dehydromonocrotaline (DHM), is believed to be responsible for MCT toxicity[9, 10]. DHM is highly active and can react with water to form a less toxic but relatively stable metabolite, 6,7-dihydro-7-hydroxy-1-hydroxymethyl-5*H*-pyrrolizine (DHP)[11]. These two metabolites can either rapidly form bound pyrroles by reacting with other cellular macromolecules, leading to toxicity, or react with glutathione (GSH) to form GSH conjugates including 7-glutathionyl-6,7-dihydro-1-hydroxymethyl-5*H*-pyrrolizine (GSH-DHP) and 7,9-diglutathionyl-6,7-dihydro-1-hydroxymethyl-5*H*-pyrrolizine (diGSH-DHP)[12–14].

Hepatic cytochrome P450s, such as CYP3A, CYP2B and CYP2C, are involved in the metabolic activation and hepatotoxicity and pneumotoxicity of MCT[1]. However, the precise role of hepatic metabolic activation of MCT in MCT-induced renal toxicity has not been well established. Cytochrome P450s are the most important xenobiotic-metabolizing enzymes and participate in the metabolism of most foreign

* To whom correspondence should be addressed.
E-mail xmqi@cdser.simm.ac.cn (Xin-ming QI);
jren@cdser.simm.ac.cn (Jin REN)
Received 2013-04-26 Accepted 2013-09-09

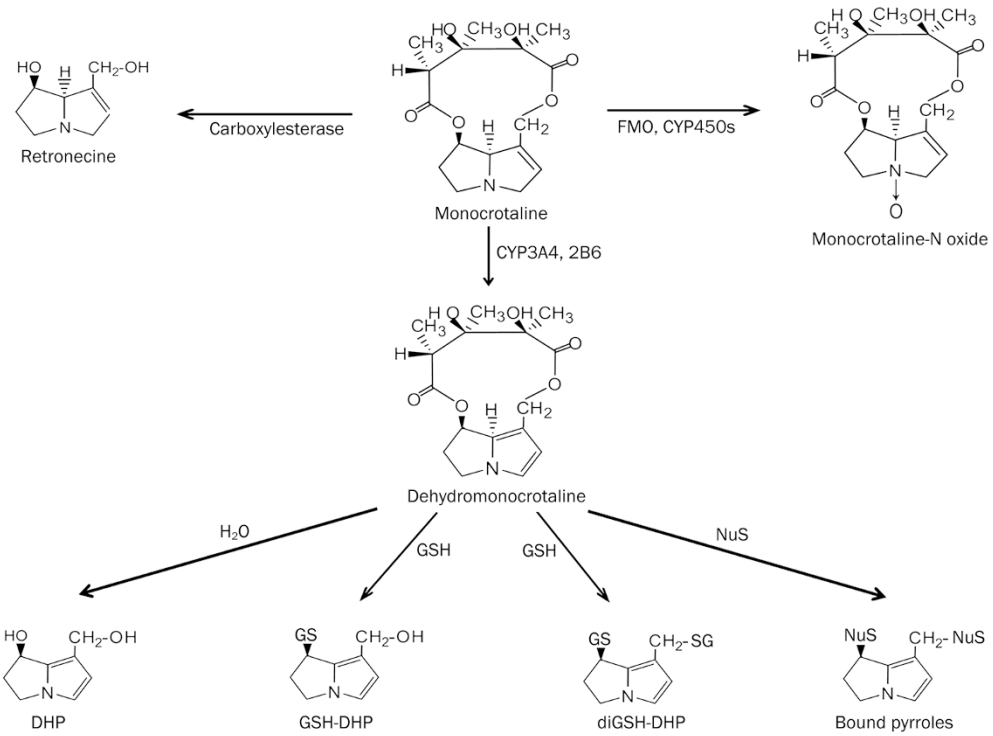

Figure 1. Scheme of the metabolic pathway of monocrotaline (MCT). MCT is mainly metabolized in three pathways. The detoxification pathways include hydrolysis by carboxylesterase to form retronecine and N-oxidation by FMO and CYP450s to form monocrotaline N-oxide (MNO). The metabolic activation of MCT occurs via dehydrogenation primarily, by CYP3A4 and CYP2B6, to form dehydromonocrotaline (DHM), which is highly active. It can react with water to form DHP and conjugate with nucleophiles to form adducts such as GSH-DHP, diGSH-DHP, and bound pyrroles.

chemicals[15]. In addition to the abundant cytochrome P450s in the liver, it is believed that various extrahepatic cytochrome P450s also contribute to xenobiotic biotransformation[16]. A unique mouse model has been developed in which the cytochrome P450 reductase (*Cpr*) gene encoding the obligate redox partner for all microsomal cytochrome P450s is deleted specifically in hepatocytes, resulting in the loss of ~95% of microsomal activity in hepatocytes. Such mice are called liver-*Cpr*-null (Null) mice[17]. Recently, this model has been used in a number of studies to investigate the role of hepatic metabolism in the extrahepatic toxicity of chemicals or drugs[18, 19].

Using this unique mouse model together with a pharmacologic inhibition method, we found that MCT-induced apoptosis of renal tubular cells and LSEC injury are dependent on hepatic cytochrome P450s. Further pharmacokinetic analysis showed that hepatic P450s contribute to the clearance and distribution of MCT and its metabolites in the kidney. Thus, we provide the evidence that hepatic cytochrome P450-mediated metabolic activation plays a critical role in MCT-induced kidney toxicity.

Materials and methods

Materials

MCT and retrorsine (RTS) were purchased from Sigma (St Louis, MO, USA). GSH was purchased from Beyotime (Haimen, China). GSH-DHP and diGSH-DHP were obtained by *o*-chloranil oxidation of MCT to DHM with limited or excess amounts of GSH, respectively[20, 21]. Monocrotaline N-oxide (MNO) and retronecine (RET) were prepared as previously described[22, 23]. All other chemicals were of reagent grade and commercially available; they were purchased from Sinopharm (Shanghai, China).

Animal treatments

Null mice were a gift from Dr Xing-xing DING (Wadsworth Center, Albany, NY, USA). Protocols for animal breeding and genotyping were reported previously[24]. Two- to four-month-old male mice from Null and WT littermate groups of mixed C57BL/6 and 129/Sv genetic backgrounds were used in these studies. All animal experiments were approved by the Institutional Animal Care and Use Committee of the Shanghai Institute of Materia Medica (Shanghai, China). Animals were maintained at 22 °C with a 12-h on and 12-h off light cycle.

Toxicological studies

Mice were treated with a single intraperitoneal injection of MCT at 300, 400, and 500 mg/kg or saline as a control. In the KET-pretreated group, KET, as a suspension in 0.5% sodium carboxyl methyl cellulose (CMC-Na), was administered twice orally at a dose of 70 mg/kg, once at 18 h and the other 1 h before the administration of MCT. Mice were euthanized 24 h after administration of MCT. After drawing blood samples via cardiac puncture, the liver and kidneys were collected promptly and processed according to standard pathology

procedures[19]. Sections (5 μm thick) were stained with hematoxylin and eosin. For semiquantitative assessment of kidney injury, the severity of kidney lesions was graded as previously described (++, severe; + moderate; ±, mild; –, negative)[24].

The serum levels of blood alanine aminotransferase (ALT), blood urea nitrogen (BUN), and creatinine were determined with an automatic HITACHI Clinical Analyzer Model 7080 (Hitachi, Tokyo, Japan). The concentration of hyaluronic acid (HA) in the serum was measured with an ELISA kit (Shanghai Xitang Biotechnology Co, Shanghai, China) according to the manufacturer's instructions.

Toxicokinetics studies

Mice were treated with a single intraperitoneal injection of MCT at 400 or 500 mg/kg. To determine the levels of MCT and its metabolites in the plasma, the blood samples were collected in heparin-coated capillaries by tail bleeding at 10 min, 30 min, and 1, 2, 4, 8, 12, or 24 h after dosing. Following centrifugation at 4000×*g* for 5 min at 4 °C, the plasma was transferred to a clean tube and kept at -80 °C until analysis. To determine the tissue distribution of MCT and its metabolites, the animals were sacrificed 1 h after MCT administration. Tissues, including the liver, kidney, and lung, were collected and homogenized in double-distilled H_2O (4 mL/g tissue). The homogenate was separated by centrifugation at 18 000×*g* for 10 min; the pellets were discarded, and the supernatants were frozen at -80 °C until use. For determination of GSH conjugates, bile was collected at 10 min, 30 min, and 1, 2, 3, 4, 5, or 6 h after MCT treatment via bile duct cannulation.

Sample treatment for liquid chromatography-mass spectrometry (LC-MS) analysis

Plasma and tissue homogenates were thawed and vortexed for 10 s. RTS was added to the samples as an internal standard, and 20% NH_3-H_2O was then added, followed by extraction with *n*-butanol. The extraction was dried using a centrifugal vacuum concentrator. The residue was reconstituted into 100 μL of 15% methanol in mobile phase A (5 mmol/L ammonium acetate with 0.1% acetic acid), vortexed, and centrifuged at 18 000×*g* for 5 min. The supernatant was then transferred to vials, and 20 μL was injected into the column for LC-MS/MS analysis.

Bile samples were mixed with 3 volumes of methanol and spun at 18 000×*g* for 5 min. The supernatants were mixed with 4 volumes of mobile phase A, filtered with a disposable filter unit, and analyzed by LC-MS/MS.

LC-MS/MS and operating conditions

The quantification of MCT and its metabolites was performed on an HPLC-ESI-MS system (Shimadzu LCMS-2010EV, Tokyo, Japan). Separation was performed on a Waters symmetry C18 column. Mobile phases A and B (acetonitrile) were used with gradient elution as follows: 0–8 min, 95%–40% A; 8–9 min, 40%–95% A; 9–12 min, 95% A. The flow rate was 0.2 mL/min. Positive electrospray ionization and multiple reaction monitoring (MRM) were performed to simultaneously monitor MCT, MNO, RTS, and RET ions at *m/z* 326/120, 342/137, 352/120, and 156/80, respectively. GSH-DHP and diGSH-DHP were analyzed in the negative electrospray ionization mode with selected ion monitoring (SIM) at *m/z* 441 and 730, respectively. Interface voltage was 4.5 kV. The desolvation line and heat block temperatures were set at 250 °C and 400 °C. The nebulization gas was set to 3 L/h with the cone gas at 50 L/h. The detector voltage was set at 1.72 kV.

For MCT, the lower limit of quantification (LLOQ) was 5 ng/mL in the plasma, liver, kidney and lung. The intra- and inter-day precisions as assessed by the relative standard deviation (RSD) were less than 10.44% and 12.49%, respectively, for plasma samples, 8.51% and 9.74% for liver samples, 9.41% and 9.02% for kidney samples, and 10.62% and 11.7% for lung samples. The mean extraction recoveries were no less than 93.17%, 95.17%, 96.02%, and 97.11% for plasma, liver, kidney and lung samples, respectively.

For MNO, the LLOQ was 5 ng/mL in the plasma, liver, kidney and lung. The intra- and inter-day precisions assessed using the RSD were less than 11.02% and 7.92% for plasma samples, 8.55% and 9.72% for liver samples, 8.13% and 10.05% for kidney samples, and 7.04% and 8.95% for lung samples, respectively. The mean extraction recoveries were no less than 70.23%, 73.12%, 74.83%, and 75.51% for plasma, liver, kidney and lung samples, respectively.

For RET, the LLOQ was 40 ng/mL in the plasma, liver, kidney and lung. The intra- and inter-day precisions were less than 7.11% and 13.20% for plasma samples, 9.12% and 12.77% for liver samples, 9.47% and 13.87% for kidney samples, and 8.25% and 10.38% for lung samples, respectively. The mean extraction recoveries were no less than 56.17%, 58.02%, 58.8%, and 60.7% for plasma, liver, kidney and lung samples, respectively.

Determination of tissue-bound pyrroles

Total tissue-bound pyrroles were estimated by modification of a reported method[13]. Briefly, the samples were homogenized in 5 volumes of acetone and centrifuged at 900×*g* for 5 min. After washing with absolute ethanol, the pellets were reconstituted in 5 volumes of 2% acidic silver nitrate ethanol solution and shaken for 30 min followed by centrifugation. The resulting supernatant was reacted with 4-dimethylaminobenzaldehyde (*v/v* 4:1) in ethanol containing 1% perchloric acid at 55 °C for 10 min. The absorbance of the sample was measured at both 562 and 625 nm. Adjusted absorbance (A) was determined as A=1.1 ($A_{562\ nm}$–$A_{625\ nm}$). The concentration of bound pyrroles was calculated using a molar absorptivity of 60 000.

Statistical analysis

Data are presented as the mean±SD, and significant differences were identified by Student's *t*-test or one-way analysis of variance (ANOVA) followed by Tukey's *post hoc* test. Differences were considered significant at P<0.05.

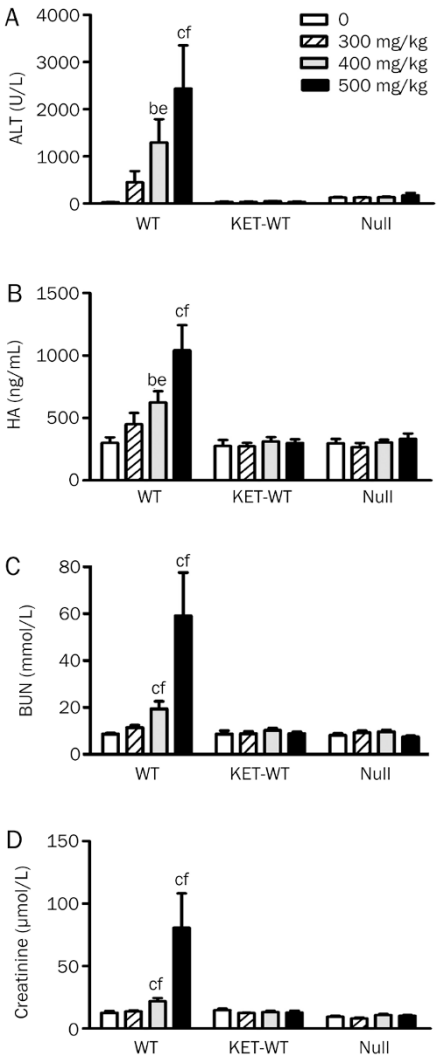

Figure 2. Comparison of serum ALT, HA, BUN, and creatinine levels in the WT, KET-WT, and Null mice. All mice received a single intraperitoneal injection of 300, 400, and 500 mg/kg MCT or saline after overnight fasting. Serum levels of ALT (A), HA (B), BUN (C), and creatinine (D) were determined in WT, KET-WT and Null mice 24 h after MCT or saline administration. Values presented are mean±SD. n=5. ^{b}P<0.05, ^{c}P<0.01 versus control WT mice. ^{e}P<0.05, ^{f}P<0.01 versus KET-WT mice treated with MCT.

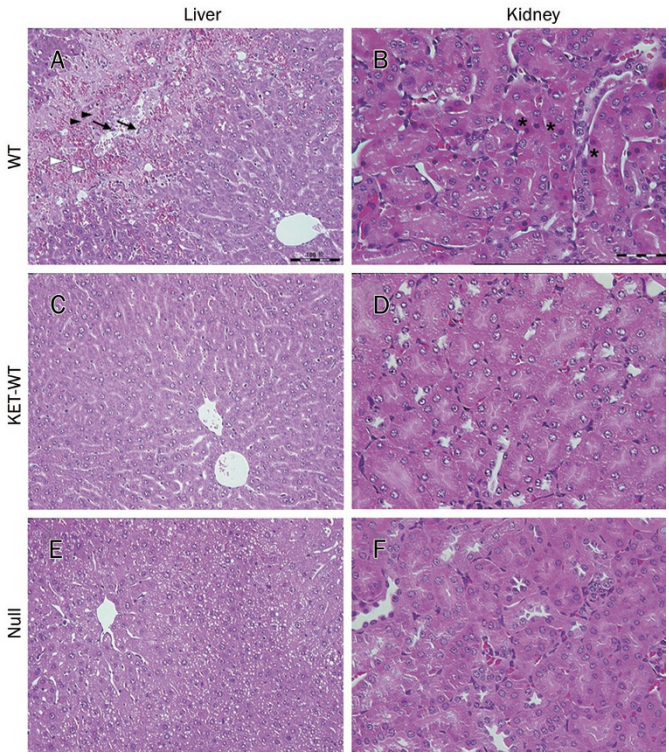

Figure 3. Comparison of liver and kidney lesions in WT, KET-WT, and Null mice induced by MCT. All mice received a single intraperitoneal injection of MCT at 500 mg/kg after overnight fasting. Histological examination of the liver of MCT-treated WT (A), KET-WT (C), and Null (E) mice and kidneys of MCT-treated WT (B), KET-WT (D) and Null (F) mice 24 h after MCT administration (HE staining). The KET-WT group was pretreated with 70 mg/kg KET twice prior to MCT injection. Black arrows: liver sinusoidal endothelial cell detachment; black arrow heads: focal hepatocyte necrosis; blank arrow heads: hemorrhage; stars: renal tubular cell apoptosis. Scale bars, 100 μm for liver, 50 μm for kidney.

Results

Abolished hepatic and renal toxicity of MCT in Null and KET-WT mice

MCT-induced toxicity was examined in Null, WT, and KET-WT mice 24 h after a single intraperitoneal injection at 300, 400, or 500 mg/kg. Serum biochemical analysis showed dose-dependent increases in serum levels of ALT, HA (a specific marker for endothelial cell injury), BUN and Cre in WT mice after treatment, whereas no changes were observed in Null and KET-WT mice (Figure 2). Histologically, 24 h after 500 mg/kg MCT injection, WT mice developed severe liver injury, such as hepatocyte necrosis, endothelial cell detachment, and severe hemorrhage (Figure 3A), and moderate kidney injury, which was characterized by renal tubular cell apoptosis (Figure 3B). However, no lesions were observed in the liver and kidney of Null or KET-WT mice (Figure 3C–3F). The severity

Table 1. Extent of tissue injury in the WT, Null, KET-WT mice induced by MCT.

Group	Tissue	Number of mice in each group			
		–	±	+	++
WT	Liver	0	0	1	5
	Kidney	2	1	3	0
Null	Liver	6	0	0	0
	Kidney	6	0	0	0
KET-WT	Liver	6	0	0	0
	kidney	6	0	0	0

All mice were treated with a single intraperitoneal injection of MCT at 500 mg/kg. Histopathology of the liver, kidney was examined 24 h after MCT treatment. The severity of lesions was graded as: ++, severe; +, moderate; ±, mild; –, negative.

of liver and kidney damage were graded among the WT, KET-WT, and Null mice (Table 1). These results indicate that inactivation of hepatic cytochrome P450s by *Cpr* knockout (Null mice) or KET pretreatment protected mice from MCT-induced injury to hepatocytes, LSECs, and kidneys.

Increased plasma content and tissue distribution of MCT in Null and KET-WT mice

The contribution of hepatic P450s to MCT metabolism was investigated *in vivo* by comparing the plasma and tissue contents of MCT among WT, Null, and KET-WT mice after a single intraperitoneal injection of MCT at 400 or 500 mg/kg. Typical LC/MS chromatograms are shown in Figure 4. Compared with WT mice, there was a significant increase in the plasma MCT levels of Null and KET-WT mice at 1 and 2 h after treatment with MCT (Figure 5A, 5B). The area under the curve (AUC) of plasma MCT in Null and KET-WT mice was markedly higher than that in WT mice (Table 2). The tissue MCT levels showed that, compared with WT mice, the MCT levels markedly increased in the liver, kidney and lung of Null and KET-WT mice 1 h after dosing (Figure 5C, 5D). Taken together, these results suggest that the inactivation of hepatic P450 or KET pretreatment compromised the metabolism of MCT *in vivo*.

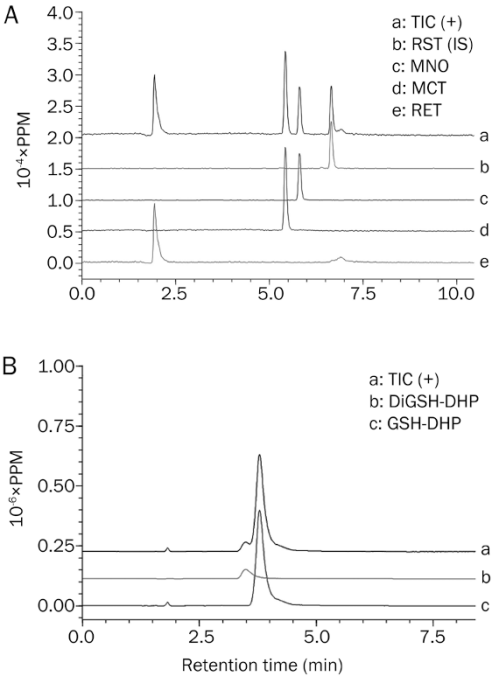

Figure 4. Typical LC-MS chromatograms of MCT, MNO, and RET in the plasma (A) and GSH-DHP, diGSH-DHP in bile (B). TIC, total ion cluster.

Diminished levels of MNO and increased levels of RET in Null and KET-WT mice

MNO and RET are important detoxified metabolites of MCT. To examine whether decreased MCT toxicity in Null and KET-WT mice was correlated with changes in the contents of these

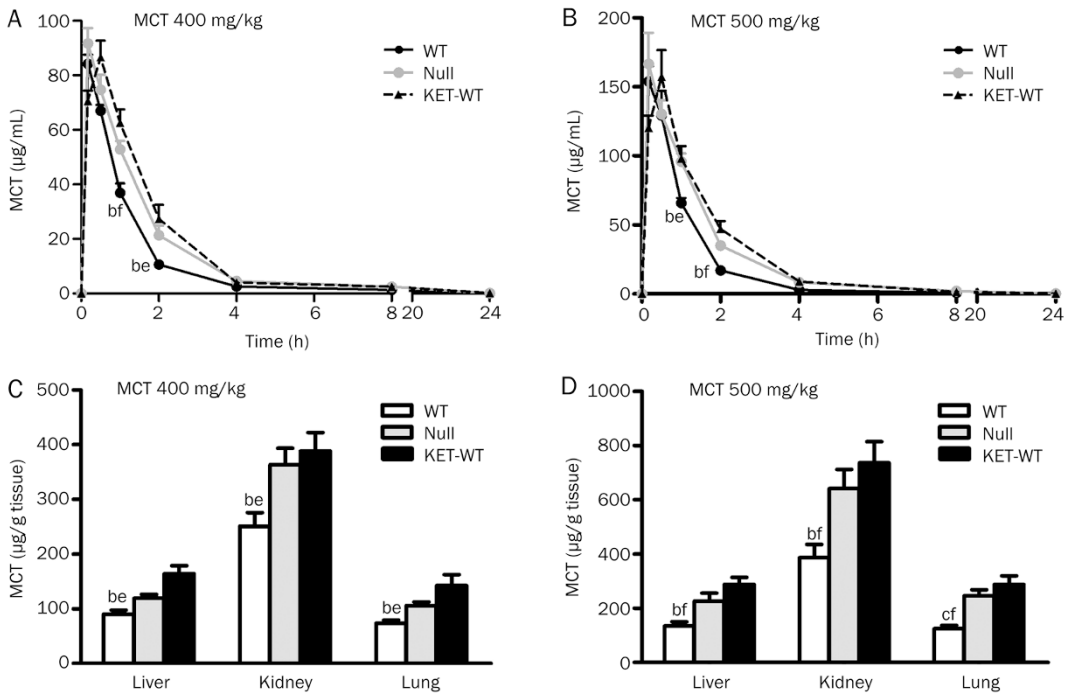

Figure 5. The levels of MCT in plasma and tissues of WT, Null, and KET-WT mice. All mice were fasted overnight before a single intraperitoneal injection of 400 or 500 mg/kg MCT. MCT levels in the plasma at various time points after treatment with 400 (A) or 500 mg/kg MCT (B). MCT contents in the liver, kidney and lung 1 h after treatment with 400 (C) or 500 mg/kg MCT (D). Values presented are mean±SD. n=5. ^{b}P<0.05, ^{c}P<0.01 versus Null mice. ^{e}P<0.05, ^{f}P<0.01 versus KET-WT mice.

Table 2. Pharmacokinetic parameters for plasma MCT, MNO, RET, and bile GSH conjugates in WT, Null, and KET-WT mice.

		$T_{1/2}$ (h)	T_{max} (h)	C_{max} (μg/mL)	AUC [(μg/mL)·h]
MCT	WT	2.68±0.22	0.24±0.15	155.14±26.04	185.28±30.98[cf]
	Null	2.53±0.21	0.24±0.15	169.07±49.62	267.62±37.05
	KET-WT	2.50±0.24	0.54±0.28	162.52±32.58	282.06±53.05
MNO	WT	3.02±0.16	1.0±0	2.95±0.17[cf]	7.49±0.69[cf]
	Null	4.90±2.15	0.92±0.20	0.77±0.14	2.86±0.30
	KET-WT	5.4±1.26	1.83±0.41	0.39±0.096	1.82±0.29
RET	WT	0.72±0.11	0.17±0	0.46±0.12	0.31±0.03[be]
	Null	0.75±0.06	0.23±0	0.40±0.09	0.39±0.04
	KET-WT	0.79±0.18	0.17±0	0.46±0.07	0.38±0.05
GSH-DHP	WT	2.73±1.12	1.00±0	819.25±68.95	2545.85±214.08[cf]
	Null	1.29±0.20	1.00±0	168.76±44.86	381.12±67.42
	KET-WT	N/A	3.00±0	273.73±66.57	787.25±129.67
diGSH-DHP	WT	1.46±0.22	1.0±0	184.15±33.94	393.89±66.78[cf]
	Null	1.76±0.54	1.0±0	23.26±4.20	43.89±2.95
	KET-WT	3.34±0.80	2.75±0.50	23.32±5.46	71.26±16.98

Plasma MCT, MNO, RET, and bile GSH-DHP, diGSH-DHP levels after the injection of 500 mg/kg MCT were used to calculate pharmacokinetic parameters, including C_{max} (the maximum concentration), T_{max} (time to reach C_{max}), AUC (area under the curve), $T_{1/2}$ (the elimination half life). Data are mean±SD. n=5. [b]P<0.05, [c]P<0.01 versus Null mice. [e]P<0.05, [f]P<0.01 versus KET-WT mice. NA, not applicable.

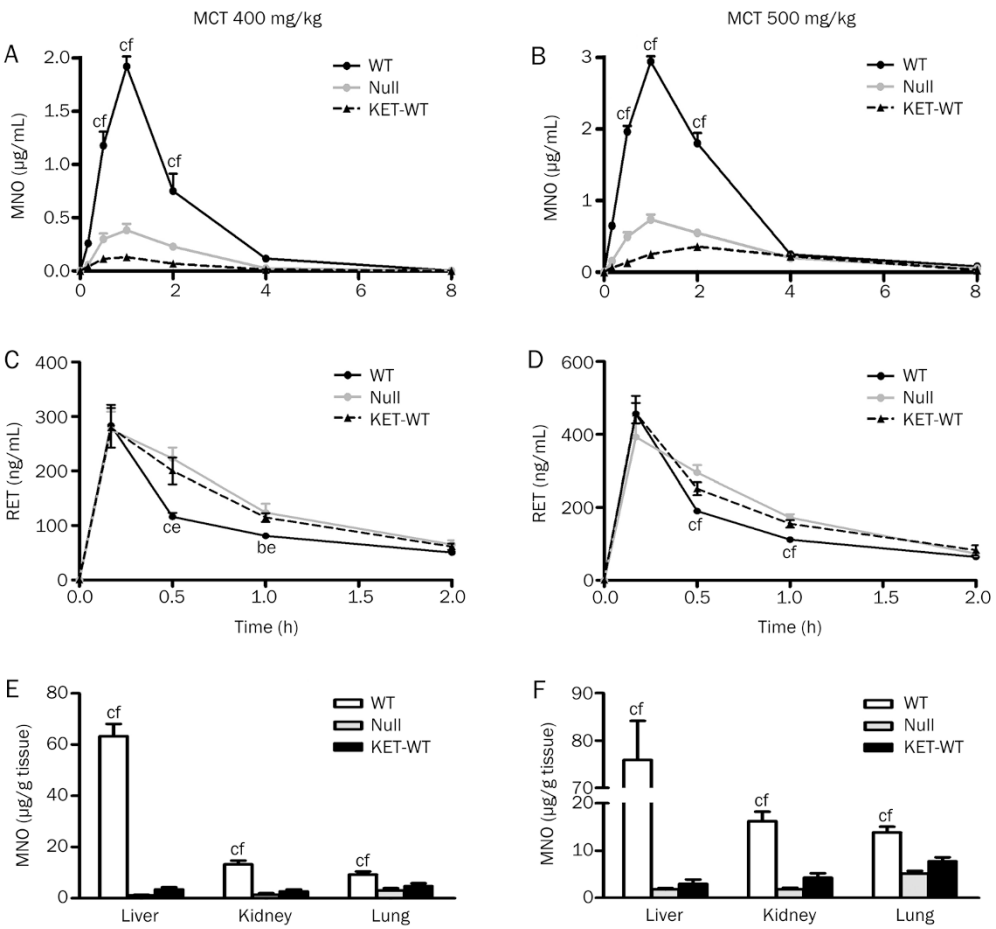

Figure 6. The plasma levels of MNO and RET and tissue levels of MNO in WT, Null and KET-WT mice. All mice were fasted overnight before a single intraperitoneal injection of MCT at 400 or 500 mg/kg. MNO levels in the plasma at various time points after treatment with 400 (A) or 500 mg/kg MCT (B). RET levels in the plasma at various time points after treatment with 400 (C) or 500 mg/kg MCT (D). MNO levels in the liver, kidney and lung 1 h after treatment with 400 (E) or 500 mg/kg MCT (F). Values presented are mean±SD. n=5. [b]P<0.05, [c]P<0.01 versus Null mice. [e]P<0.01, [f]P<0.01 versus KET-WT mice.

metabolites, we determined the levels of MNO and RET in the plasma and tissues of mice treated with MCT at 400 and 500 mg/kg. We found that plasma MNO levels were significantly lower in Null and KET-WT mice than in WT mice at time points ranging from 30 min to 2 h (Figure 6A, 6B). Similarly, the levels of MNO in the liver, kidney, and lung of Null and KET-WT mice were significantly decreased compared with WT mice (Figure 6E, 6F). As shown in Table 2, there was a significant decrease in the C_{max} and AUC of MNO in Null and KET-WT mice compared to those in WT mice. The plasma RET levels were significantly higher in Null and KET-WT mice at 30 min and 1 h after MCT administration compared to those in WT mice (Figure 6C, 6D). Unexpectedly, RET levels in tissues could not be detected in our test conditions, possibly because the RET contents may have been below the detection limit.

Inhibition of metabolic activation of MCT in Null and KET-WT mice

The toxicity of MCT is associated with the toxic metabolites DHM and DHP. However, they are very reactive and easily form adducts with endogenous nucleophilic macromolecules. To examine the metabolic activation of MCT, we determined the levels of DHP adducts including GSH-DHP, diGSH-DHP, and tissue-bound pyrroles in mice after a single intraperitoneal injection of MCT at 400 or 500 mg/kg. Compared with WT mice, the amount of tissue-bound pyrroles decreased significantly in the liver, kidney and lung of Null and KET-WT mice 1 h after treatment with MCT (Figure 7A, 7B), accompanied by a marked decrease in the levels of bile GSH-DHP and diGSH-DHP from 30 min to 2 h (Figure 7C–7F). Consistent with these results, the AUCs of GSH-DHP and diGSH-DHP were significantly lower in Null and KET-WT mice (Table 2). Notice-

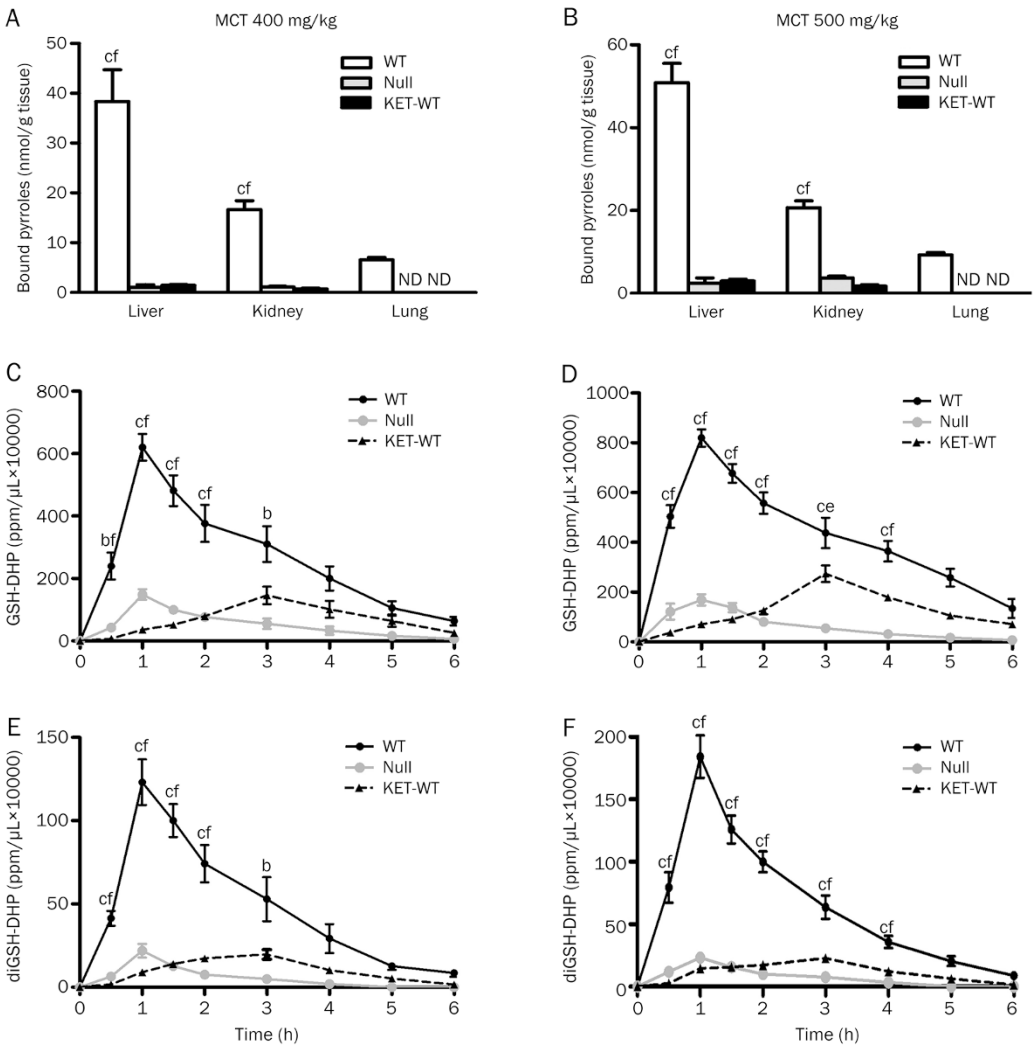

Figure 7. The levels of tissue-bound pyrroles and bile GSH-DHP and diGSH-DHP in WT, Null, and KET-WT mice. The tissues were collected from mice at 1 h after a single injection of MCT at 400 or 500 mg/kg. Bound pyrrole levels in the liver, kidney and lung 1 h after treatment with 400 (A) or 500 mg/kg MCT (B). GSH-DHP in the bile at various time points after treatment with 400 (C) or 500 mg/kg MCT (D). diGSH-DHP levels in the bile at various time points after treatment with 400 (E) or 500 mg/kg MCT (F). Values presented are mean±SD. n=5. ^{b}P<0.05, ^{c}P<0.01 versus Null mice. ^{e}P<0.05, ^{f}P<0.01 versus KET-WT mice.

ably, the bile levels of GSH-DHP and diGSH-DHP started to decrease in WT mice 1 h after dosing, whereas those in KET-WT mice started to decline approximately 3 h after the injection. Altogether, these results suggest that the inactivation of hepatic cytochrome P450s or KET pretreatment inhibited the metabolic activation of MCT.

Discussion

The ingestion of MCT causes intra- and extrahepatic toxicity after metabolic activation of MCT. It has been reported that MCT-induced pneumotoxicity is tightly linked to metabolic activation in the liver, based on studies of *in vitro* and *ex vivo* perfusion[9, 25]. Here, we provide direct evidence that hepatocyte P450s play a critical role in the production of active metabolites in the extrahepatic tissues of mice. Furthermore, we demonstrated that liver-specific P450s are responsible for MCT-induced injury to the kidney as well as LSECs.

Dehydrogenation is an essential metabolic activation step for the rapid clearance of MCT *in vivo*[1]. The inactivation of hepatic cytochrome P450s totally abolished MCT-induced toxicity, which strongly suggests a major role of hepatic cytochrome P450s in the metabolic activation and toxicity of MCT. Cyp3a, Cyp2b, and Cyp2c have been reported to be involved in the metabolic activation of MCT[1]. In sheep, hamsters and guinea pigs, Cyp2b and Cyp2c play a role in the bioactivation of MCT[1], while in rats and mice, multiple studies have shown a major role for Cyp3a in the formation of reactive pyrroles[25–28]. Anti-Cyp3a antibody almost completely inhibits the formation of reactive pyrroles (94% inhibition)[25]. In this study, as a highly selective inhibitor of Cyp3a[29], KET, markedly suppressed the metabolic activation and toxicity of MCT. Taken together, these data suggest that hepatic Cyp3a, the most abundant isoenzyme of cytochrome P450s in the liver[30], may play a major role in the metabolic activation and toxicity of MCT.

In contrast to a previous report that MCT induces nephrotoxicity, as demonstrated by necrotic changes in the glomeruli and hemosiderin granules in tubular epithelial cells, as well as focal endothelial cell detachment[31, 32], we found that MCT caused apoptosis of renal tubular cells in WT mice (Figure 2B). This disparity might be due to differences in species, route of MCT administration or sampling time. In Null mice, LSEC injury was abolished (Figure 2B, 3E), indicating that the metabolic activation of MCT in hepatocytes was responsible for MCT-induced LSECs toxicity. Moreover, the higher sensitivity of LSECs to MCT may be explained by the low capacity of these cells to synthesize GSH, which results in reduced GSH detoxification[33].

In our study, the dramatically decreased levels of bound pyrroles in the kidneys of Null mice indicated that the bioactivation of MCT in liver contributes to the production of bound pyrroles in the kidneys. This point is supported by a report that DHM and DHP, highly reactive metabolites of MCT, can reach extrahepatic tissues such as the kidney and lung[34].

Several previous studies have reported that treatment with a CYP3A inhibitor cannot completely abolish the bioactivation of PAs[35, 36]. Similarly, in our study, bound pyrroles in the liver and kidney were not totally abolished in KET-WT mice, which could be attributed to the incomplete inhibition of Cyp3a in hepatocytes by KET. Likewise, the inactivation of hepatic P450s in Null mice did not totally abolish the formation of GSH conjugates and bound pyrroles, which may be for the following reasons: (1) In Null mice, Cpr knockout does not completely abolish the microsomal activity; approximately 5% microsomal activity remains, with cytochrome b5 as the electron donor[37, 38]. (2) Kidney microsomes also have the capacity to metabolically activate PAs[36]. (3) Cyp3a, which is abundant in the small intestine, may also be implicated in the generation of active metabolites in the liver and kidney in Null mice[39].

MNO and RET are important detoxified metabolites of MCT. The plasma and tissue levels of MNO were markedly decreased in Null mice, indicating that hepatic P450s greatly contributed to the production of MNO. Similarly, the levels of MNO were significantly decreased in KET-WT mice (Figure 6A, 6C). Considering the importance of Cyp3a in the N-oxidation of PAs[1], our results suggest that hepatic Cyp3a might play an important role in N-oxidation of MCT *in vivo*. The increases in the plasma levels of RET in KET-WT and Null mice might be due to the increased processing of MCT by enzymes such as carboxylesterase.

In summary, hepatic P450s play an important role in the metabolism and toxicity of MCT *in vivo*. Because considerable polymorphisms of cytochrome P450s have been observed in humans[40], our results suggest that populations with higher cytochrome P450 activities, especially CYP3A, may have a higher risk for toxicity induced by MCT or other PAs. Our findings provide new insights into the mechanisms of MCT-induced LSEC damage and nephrotoxicity and possible new approaches for the treatment or prevention of PA-induced toxicity.

Acknowledgements

This work was supported by Key Projects of National Science and Technology Pillar Program (2012ZX09301001-006 and 2012zx09302003) and the Public Service Platform Project of Shanghai Science and Technology Committee (11DZ2292500) We thank Prof Yi-zheng WANG and Guo-yu PAN for helpful advice.

Author contribution

Jun YAO, Xin-ming QI, and Jin REN designed the experiment; Jun YAO, Cheng-gang LI, Chen-chen FENG, Chun-zhu LI, and Man GAO performed the research; Jun YAO wrote this paper; Yang LUAN purchased the reagents; Jun YAO, Li-kun GONG, and Xin-ming QI analyzed data; Xin-ming QI and Jin REN revised the manuscript.

References

1 Fu PP, Xia Q, Lin G, Chou MW. Pyrrolizidine alkaloids — genotoxicity, metabolism enzymes, metabolic activation, and mechanisms. Drug Metab Rev 2004; 36: 1–55.

2 Kempf M, Reinhard A, Beuerle T. Pyrrolizidine alkaloids (PAs) in honey

and pollen-legal regulation of PA levels in food and animal feed required. Mol Nutr Food Res 2010; 54: 158–68.
3 Roeder E. Medicinal plants in Europe containing pyrrolizidine alkaloids. Die Pharmazie 1995; 50: 83–98.
4 Copple BL, Banes A, Ganey PE, Roth RA. Endothelial cell injury and fibrin deposition in rat liver after monocrotaline exposure. Toxicol Sci 2002; 65: 309–18.
5 DeLeve LD, McCuskey RS, Wang X, Hu L, McCuskey MK, Epstein RB, *et al*. Characterization of a reproducible rat model of hepatic veno-occlusive disease. Hepatology 1999; 29: 1779–91.
6 Mattocks AR. Chemistry and toxicology of pyrrolizidine alkaloids. London, Orlando Fla: Academic Press; 1986.
7 Petzinger E. Pyrrolizidine alkaloids and seneciosis in farm animals. Part 1: occurrence, chemistry and toxicology. Tierarztl Prax Ausg G Grosstiere Nutztiere 2011; 39: 221–30.
8 Stegelmeier BL, Edgar JA, Colegate SM, Gardner DR, Schoch TK, Coulombe RA, *et al*. Pyrrolizidine alkaloid plants, metabolism and toxicity. J Nat Toxins 1999; 8: 95–116.
9 Lafranconi WM, Huxtable RJ. Hepatic metabolism and pulmonary toxicity of monocrotaline using isolated perfused liver and lung. Biochem Pharmacol 1984; 33: 2479–84.
10 Pan LC, Wilson DW, Lame MW, Jones AD, Segall HJ. COR pulmonale is caused by monocrotaline and dehydromonocrotaline, but not by glutathione or cysteine conjugates of dihydropyrrolizine. Toxicol Appl Pharmacol 1993; 118: 87–97.
11 Mattocks AR. Dihydropyrrolizine derivatives from unsaturated pyrrolizidine alkaloids. J Chem Soc C 1969; (8): 1155–62.
12 Lin G, Cui YY, Hawes EM. Characterization of rat liver microsomal metabolites of clivorine, an hepatotoxic otonecine-type pyrrolizidine alkaloid. Drug Metab Dispos 2000; 28: 1475–83.
13 Lin G, Wang JY, Li N, Li M, Gao H, Ji YA, *et al*. Hepatic sinusoidal obstruction syndrome associated with consumption of *Gynura segetum*. J Hepatol 2011; 54: 666–73.
14 Yan CC, Huxtable RJ. Effects of monocrotaline, a pyrrolizidine alkaloid, on glutathione metabolism in the rat. Biochem Pharmacol 1996; 51: 375–9.
15 Rooney PH, Telfer C, McFadyen MC, Melvin WT, Murray GI. The role of cytochrome P450 in cytotoxic bioactivation: future therapeutic directions. Curr Cancer Drug Targets 2004; 4: 257–65.
16 Bernauer U, Heinrich-Hirsch B, Tonnies M, Peter–Matthias W, Gundert-Remy U. Characterisation of the xenobiotic–metabolizing cytochrome P450 expression pattern in human lung tissue by immunochemical and activity determination. Toxicol Lett 2006; 164: 278–88.
17 Gu J, Weng Y, Zhang QY, Cui H, Behr M, Wu L, *et al*. Liver-specific deletion of the NADPH-cytochrome P450 reductase gene: impact on plasma cholesterol homeostasis and the function and regulation of microsomal cytochrome P450 and heme oxygenase. J Biol Chem 2003; 278: 25895–901.
18 Gu J, Cui H, Behr M, Zhang L, Zhang QY, Yang W, *et al*. *In vivo* mechanisms of tissue-selective drug toxicity: effects of liver-specific knockout of the NADPH-cytochrome P450 reductase gene on acetaminophen toxicity in kidney, lung, and nasal mucosa. Mol Pharmacol 2005; 67: 623–30.
19 Xiao Y, Ge M, Xue X, Wang C, Wang H, Wu X, *et al*. Hepatic cytochrome P450s metabolize aristolochic acid and reduce its kidney toxicity. Kidney Int 2008; 73: 1231–9.
20 Mattocks AR, Croswell S, Jukes R, Huxtable RJ. Identity of a biliary metabolite formed from monocrotaline in isolated, perfused rat liver. Toxicon 1991; 29: 409–15.
21 Mattocks AR, Jukes R, Brown J. Simple procedures for preparing putative toxic metabolites of pyrrolizidine alkaloids. Toxicon 1989; 27: 561–7.
22 Chou MW, Wang YP, Yan J, Yang YC, Beger RD, Williams LD, *et al*. Riddelliine N-oxide is a phytochemical and mammalian metabolite with genotoxic activity that is comparable to the parent pyrrolizidine alkaloid riddelliine. Toxicol Lett 2003; 145: 239–47.
23 Hoskins WM, Crout DH. Pyrrolizidine alkaloid analogues. Preparation of semisynthetic esters of retronecine. J Chem Soc Perkin Transact 1 1977; (5): 538–44.
24 Wu L, Gu J, Cui H, Zhang QY, Behr M, Fang C, *et al*. Transgenic mice with a hypomorphic NADPH-cytochrome P450 reductase gene: effects on development, reproduction, and microsomal cytochrome P450. J Pharmacol Exp Ther 2005; 312: 35–43.
25 Kasahara Y, Kiyatake K, Tatsumi K, Sugito K, Kakusaka I, Yamagata S, *et al*. Bioactivation of monocrotaline by P-450 3A in rat liver. J Cardiovasc Pharmacol 1997; 30: 124–29.
26 Reid MJ, Lame MW, Morin D, Wilson DW, Segall HJ. Involvement of cytochrome P450 3A in the metabolism and covalent binding of ^{14}C-monocrotaline in rat liver microsomes. J Biochem Mol Toxicol 1998; 12: 157–66.
27 Lin G, Cui YY, Liu XQ. Gender differences in microsomal metabolic activation of hepatotoxic clivorine in rat. Chem Res Toxicol 2003; 16: 768–74.
28 Wu YM, Joseph B, Berishvili E, Kumaran V, Gupta S. Hepatocyte transplantation and drug-induced perturbations in liver cell compartments. Hepatology 2008; 47: 279–87.
29 Baldwin SJ, Bloomer JC, Smith GJ, Ayrton AD, Clarke SE, Chenery RJ. Ketoconazole and sulphaphenazole as the respective selective inhibitors of P4503A and 2C9. Xenobiotica 1995; 25: 261–70.
30 Kazuki Y, Kobayashi K, Aueviriyavit S, Oshima T, Kuroiwa Y, Tsukazaki Y, *et al*. Trans-chromosomic mice containing a human CYP3A cluster for prediction of xenobiotic metabolism in humans. Human Mol Genet 2013; 2: 578–92.
31 Hayashi Y, Lalich JJ. Renal and pulmonary alterations induced in rats by a single injection of monocrotaline. Exp Biol Med (Maywood) 1967; 124: 392–6.
32 Kurozumi T, Tanaka K, Kido M, Shoyama Y. Monocrotaline-induced renal lesions. Exp Mol Pathol 1983; 39: 377–86.
33 Wang XD, Kanel GC, DeLeve LD. Support of sinusoidal endothelial cell glutathione prevents hepatic veno-occlusive disease in the rat. Hepatology 2000; 31: 428–34.
34 Mattocks AR, Jukes R. Trapping and measurement of short-lived alkylating agents in a recirculating flow system. Chem Biol Interac 1990; 76: 19–30.
35 Xia Q, Chou MW, Kadlubar FF, Chan PC, Fu PP. Human liver microsomal metabolism and DNA adduct formation of the tumorigenic pyrrolizidine alkaloid, riddelliine. Chem Res Toxicol 2003; 16: 66–73.
36 Wang YP, Fu PP, Chou MW. Metabolic activation of the tumorigenic pyrrolizidine alkaloid, retrorsine, leading to DNA adduct formation *in vivo*. Int J Environ Res Public Health 2005; 2: 74–9.
37 Gu J, Weng Y, Zhang QY, Cui H, Behr M, Wu L, *et al*. Liver-specific deletion of the NADPH-cytochrome P450 reductase gene: impact on plasma cholesterol homeostasis and the function and regulation of microsomal cytochrome P450 and heme oxygenase. J Biol Chem 2003; 278: 25895–901.
38 Henderson CJ, Otto DM, Carrie D, Magnuson MA, McLaren AW, Rosewell I, *et al*. Inactivation of the hepatic cytochrome P450 system by conditional deletion of hepatic cytochrome P450 reductase. J Biol Chem 2003; 278: 13480–6.
39 Gibbs MA, Thummel KE, Shen DD, Kunze KL. Inhibition of cytochrome P-450 3A (CYP3A) in human intestinal and liver microsomes: comparison of Ki values and impact of CYP3A5 expression. Drug Metab Dispos 1999; 27: 180–7.
40 Westlind-Johnsson A, Malmebo S, Johansson A, Otter C, Andersson TB, Johansson I, *et al*. Comparative analysis of CYP3A expression in human liver suggests only a minor role for CYP3A5 in drug metabolism. Drug Metab Dispos 2003; 31: 755–61.